1. David UKWUNGWU[1], 2. Nora LEUNING[1], 3. Kay HAMEYER[1]

Institute of Electrical Machines (IEM), RWTH Aachen University, Germany (1)

doi:10.15199/48.2024.10.29

Simulation of the Effects of Weld-Packaging on the Electromagnetic Properties of Electrical Steel Sheets Using a Local Varying Material Model

***Abstract**. In this study, a local varying material model for the simulation of the influence of weld-packaging on the electromagnetic properties of non-oriented (NO) electrical steel sheets is presented. Welding, interlocking, clinching and gluing are typical technologies utilized during the manufacturing of electrical steel stacks of electrical machines. The mapping of the microscopic effects of weld-packaging with the macroscopic properties of the packaged core is useful for the comprehensive analysis of the effects of the process on the performance and achievable range of the electrical vehicle. The mapping will enable the understanding of the influence of welding process on the micro-structure of the utilized electrical steel. To analyze the effects of welding on the grain size of the electrical steel, five electrical steel specimens are annealed at five different temperatures. The annealed samples are then electromagnetically characterized to determine their magnetization and loss quantities. The specimens are also measured under different mechanical stress, to characterize the stress dependency of the welding process on the electromagnetic properties. This results in a model that encompasses the degree of deterioration of the electromagnetic properties by both residual stress and grain size.*

***Streszczenie.** W tym badaniu przedstawiono lokalny zmienny model materiałowy do symulacji wpływu spawania pakietów blach na właściwości elektromagnetyczne nieorientowanych (NO) blach elektrotechnicznych. Spawanie, blokowanie, zaciskanie i klejenie to typowe technologie stosowane podczas produkcji rdzeni pakietowanych z blach elektrotechnicznych maszyn elektrycznych. Mapowanie mikroskopowych efektów spawania rdzeni pakietowanych z makroskopowymi właściwościami zapakowanego rdzenia jest przydatne do kompleksowej analizy wpływu procesu na wydajność i osiągalny zasięg pojazdu elektrycznego. Mapowanie umożliwi zrozumienie wpływu procesu spawania na mikrostrukturę wykorzystanej blachy elektrotechnicznej. Aby przeanalizować wpływ spawania na wielkość ziarna blachy elektrotechnicznej, pięć próbek stali elektrotechnicznej jest wyżarzanych w pięciu różnych temperaturach. Wyżarzone próbki są następnie charakteryzowane elektromagnetycznie w celu określenia ich wielkości namagnesowania i strat. Próbki są również mierzone przy różnym naprężeniu mechanicznym, aby scharakteryzować zależność naprężeń procesu spawania od właściwości elektromagnetycznych. W rezultacie powstaje model, który obejmuje stopień pogorszenia właściwości elektromagnetycznych zarówno przez naprężenie szczątkowe, jak i wielkość ziarna. (**Symulacja wpływu pakowania zgrzewanego na właściwości elektromagnetyczne blach elektrotechnicznych przy użyciu lokalnego modelu materiału zmiennego**)*

Keywords: lamination packaging, modeling, numerical simulation, electrical steel.
Słowa kluczowe: pakowanie laminowane, modelowanie, symulacja numeryczna, stal elektrotechniczna.

Introduction

For the construction of a mechanically stable magnetic core of an electrical ac machine, the electrical steel laminations must be firmly connected. Welding, interlocking, clinching and gluing represent the current state of the art in the mechanical connection procedures of such thin steel sheets. Each of the connecting processes leads directly to the deterioration of the material's magnetic properties. Increased iron losses as well as a decreasing permeability of the electrical steel can be observed. Welding procedure is one of the most utilized packaging technologies because of its low degree of deterioration of the magnetic properties of the electrical steel sheet. During this process, the sheets are joined thermally along a seam or spot accompanied by an apparent dissipation of heat in and around the welding area. The local concentration of dissipated heat during welding leads to the thermal degradation and changes in the micro-structure (average grain size) of the electrical steel sheet. Changes in the grain size and in the residual stress in and around the weld-area lead to significant electromagnetic deterioration of the electrical steel.

In this study, a locally varying material model used in simulating the effects of weld-packaging on the electromagnetic properties of non-oriented (NO) electrical steel is presented. With the thorough understanding of the impact of welding, the development of a comprehensive application dependent method of improvement of the deterioration effects of weld-packaging will be made possible. Starting from the simulation of residual stress distributions and changes in average grain sizes attributed to weld-packaging on the basis of equivalent heat source, to the measurement of processed samples under different mechanical stress, a model representing the material degradation of weld-packaged electrical steel is introduced. Annealing processing of samples leads to different grain sizes, together with the measurements under stresses, the determination of the dependency of the electromagnetic property of the material on average grain size and residual stress is achieved. The welding procedure is modeled as an equivalent heat source. The equivalent heat source has the characteristics of a specific weld parameter with which a ring core sample will be manufactured with the aim of verifying the locally varying material model.

Experimental Approach

A non-oriented (NO) electrical steel of grade 280-30AP is utilized for this work. For the annealing process, single sheet samples (SST) of $\mathbf{180\ mm} \times \mathbf{60\ mm}$ dimensions are manufactured. For the reproducibility of this process 3 samples of each annealing temperature are produced. The temperatures utilized for the annealing process are $\mathbf{800\ ^\circ C}$, $\mathbf{900\ ^\circ C}$, $\mathbf{1000\ ^\circ C}$, $\mathbf{1100\ ^\circ C}$ and $\mathbf{1200\ ^\circ C}$. The resulting average grain sizes emanating from the annealing process are $\mathbf{80\ \mu m}$, $\mathbf{97\ \mu m}$, $\mathbf{140\ \mu m}$, $\mathbf{237\ \mu m}$, $\mathbf{277\ \mu m}$ respectively. The non-oriented (NO) electrical steel of grade 280-30AP has an average grain size of $\mathbf{78\ \mu m}$. For the model verification, spot-welded ring core laminations of inner D_i and outer D_o diameters of $\mathbf{60\ mm}$ and $\mathbf{48\ mm}$ respectively are manufactured. The specific iron loss and magnetization emanating from this sample represents the electromagnetic properties of the weld-packaged stack. The individual rings are laser cut to the aforementioned dimensions.

For the welding process, an equivalent heat source is modeled, to reproduce an energy absorption rate of $\mathbf{110\ W}$. This is the calculated absorption rate, while welding with a laser power of $\mathbf{328\ W}$, a focal position of $\mathbf{0\ mm}$ and a working pressure of $\mathbf{1\ bar}$. A multi-mode disc-laser with a focal length of $400\,\mathrm{mm}$ is utilized for the ring core packaging with the aim of verifying the model.

Measurement method

The calculation of sample geometric dimensions of the electromagnetically characterized ring samples and SST-samples utilized for this analysis are done according to DIN-IEC-60205 standard.

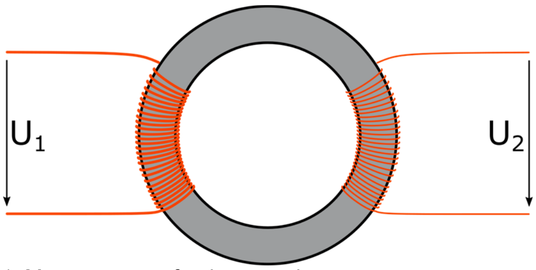

Fig 1: Measurement of a ring sample.

In the primary winding, a magnetic field is generated with the connection of a current source. This magnetic field in the primary winding induces a voltage response on the secondary winding. The electromagnetic properties are then derived from the voltage response and the geometric dimensions of the samples according to DIN-IEC-60404 standard. In Eq. 1 is the mathematical description of the induced voltage $(\overline{U_2})$ with $f, A,\ B$ and N_2 being the frequency, the cross-sectional area of the ring, the flux density and number of turns in the measuring winding respectively.

(1) $\overline{U_2} = 4 \cdot f \cdot A \cdot B \cdot N_2$

The calculation of the generated magnetic field strength *H* from the applied current *I*, number of turns N_1 on the primary winding and the magnetic length l_m is achieved with to Eq. 2.

(2) $H = \frac{N_1 \cdot I}{l_\mathrm{m}}$

Measurement Results

In this section, the magnetization values of the processed samples under different mechanical stresses are quantitatively analyzed. The universal testing machine used in the application of stress can provide forces of up to $20\,\mathrm{kN}$. This amounts to a theoretical available mechanical stress load of up to $1111\,\mathrm{MPa}$ with a $0.3\,\mathrm{mm}$ thick non-oriented (NO) electrical steel sheet cut into $180\,\mathrm{mm} \times 60\,\mathrm{mm}$ dimensions. Essentially, this device can load the sheets up to its plastic deformation stage. A symmetrical flux-guiding yoke is used in ensuring a homogeneous distribution of the magnetic field and to close the generated magnetic circuit of the SST sample. The winding of the coil directly on the sample enables the possibility of magnetizing and measuring of the macroscopic magnetic properties using a ring core tester. In Fig. 2 and 3 is the magnetization and permeability curve of the different processed samples under no stress influence at $1000\,\mathrm{Hz}$ shown. The deterioration effect of changes in the micro-structure (grain size) can be observed. With the increasing value of the average grain size (higher micro-structural degradation), a decreasing permeability value is observed. This is due to the domain wall movements that are dependent on the state of the micro-structure.

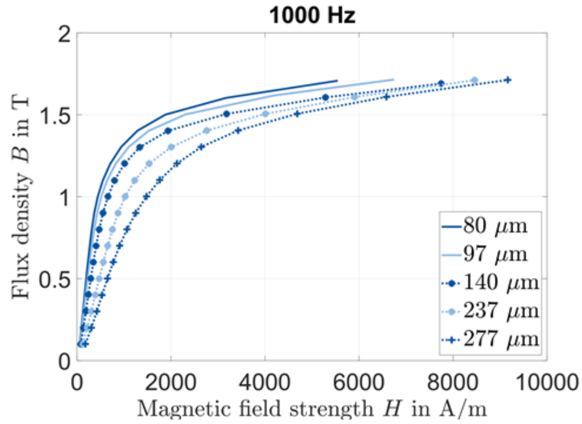

Fig 2: Magnetization at 1000 Hz

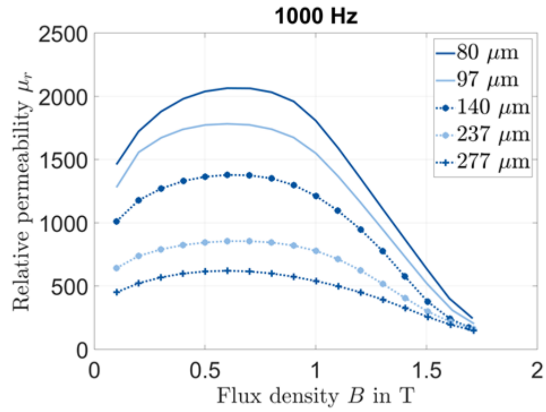

Fig 3: Relative permeability at 1000 Hz.

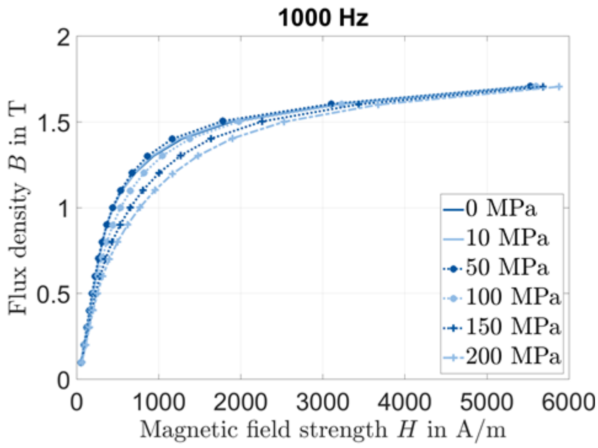

Fig 4: Magnetization at 1000 Hz

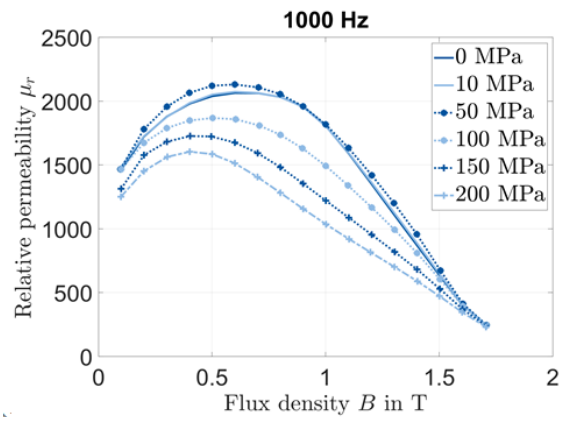

Fig 5: Relative permeability at 1000 Hz.

It is also observed that the decrease of the magnetization is pronounced on the whole low and medium flux density range. At high flux densities, a reduction in the deterioration of the magnetization is attributed to domain rotation being the main magnetization mechanism. It can also be seen, that an up to $100\,\%$ increase in the micro-structure (average grain size) will lead to an up to $40\,\%$ reduction of the maximum attainable relative permeability of the material.

The thermal energy associated with the welding process leads to the deterioration of the micro-structure (an increase in the average grain size), therefore it can be concluded that an improvement of the electromagnetic properties can be achieved with the reduction of the inputted thermal energy.

Fig. 4 and 5 depicts the magnetization and permeability curve of the different processed samples under stress influence at $1000\ \mathrm{Hz}$ and at an average grain size of $80\ \mu\mathrm{m}$. Observation of an initial improvement of the electromagnetic property is seen. Magnetic deterioration is observed at stress values higher than $60\ \mathrm{MPa}$. The degradation of the electric steel sheet under stress is seen to increase rapidly at high stress values. The Eq. 3 depicts the equivalent mathematical equation of the local changing permeability values (μ_r).

(3) $\mu_\mathrm{r}\left(d_\mathrm{grains}, \sigma\right) = \frac{B\left(d_\mathrm{grains},\sigma\right)}{\mu_0 \cdot H\left(d_\mathrm{grains},\sigma\right)}$

FEM simulation

The simulation is based on a closed simulation loop starting from the modeling of a welding procedure equivalent heat source, to the simulation of the distribution of residual stress and micro-structural (grain size) changes and the electromagnetic simulation of a geometry (ring core). The equivalent heat source is modeled from the temperature profile of welding procedure as well as the welding parameters (welding speed, beam power, degree of absorption, focal diameter, etc.). The Fig. 6 depicts the stress distribution inside the ring core. It shows an increase in the stress values and later a decrease outgoing from the weld-point.

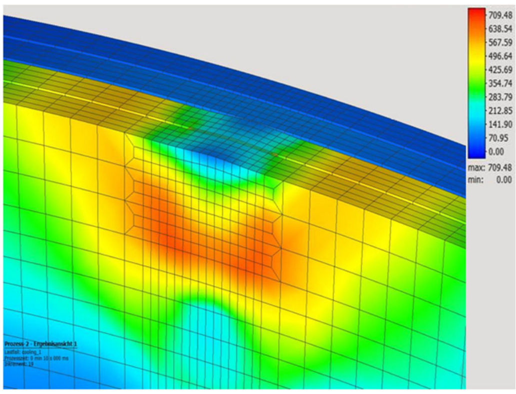

Fig 6: Simulated stress distribution.

The efficient modeling of the welding process is achieved with the mapping of the characterized electromagnetic properties at different average grain sizes and mechanical stresses to the simulated distribution of the residual stress and grain size. The calculation of the emanating grain size distribution due to weld-packaging is achieved using the micro-structure evolution simulation software (MICRESS). It uses the heat capacity and conductivity profile of the material, defined by the chemical composition of the electrical steel, in determining the mobility of the grain boundary. The micro-macro mapping of the micro-structural changes of the electrical steel sheet to the deteriorations due to weld-packaging represents the complete material model. The simulation of a ring core geometry using a local varying residual stress and grain size values is achieved with this model using the pyMOOSE simulation software.

Verification of the model

For the verification of the simulated results, ring core samples are welded with the same welding parameters of the simulated samples. A laser power of $328\ \mathrm{W}$, a focal position of $0\ \mathrm{mm}$ and a working pressure $1\ \mathrm{bar}$ are the welding parameters utilized for the simulation of the grain size and residual stress distribution as well as the weld-packaging of the manufactured core. Fig. 7 depicts the simulated and measured magnetization values of the glued and welded sample. It shows a general degradation of electromagnetic property due to weld-packaging.

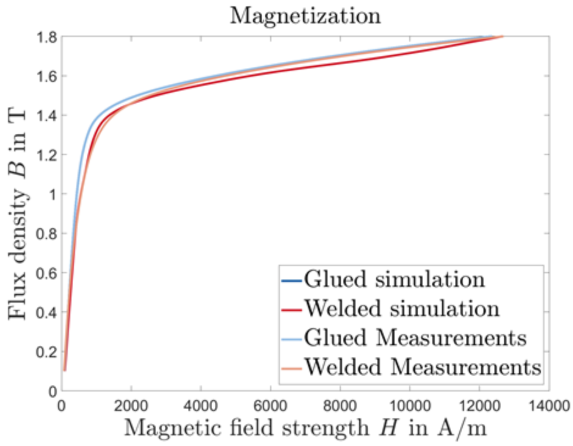

Fig 7: Magnetization curve at $1000\ Hz$.

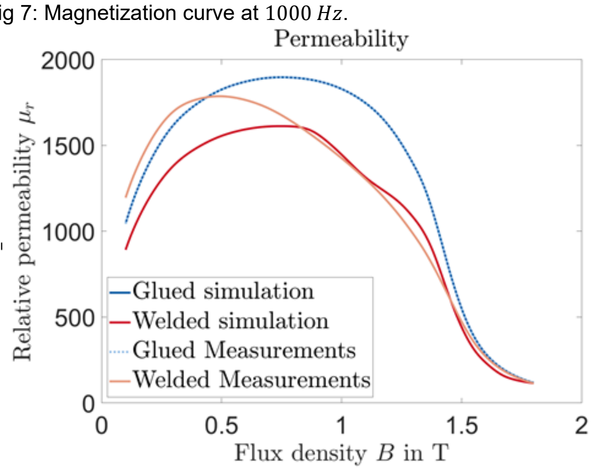

Fig 8: Relative. permeability at $1000\ Hz$.

The permeability curve in Fig. 8 shows the general reduction in the attainable values due to weld-packaging. At high flux density, a better agreement of the measured and simulated values due to the measurement accuracy of ring cores at high flux density spectrum is seen. This is due to the high accuracy of the electromagnetic measurements at these flux density values. A deterioration of the attainable permeability at low and medium flux density spectrum can be observed from the simulation result.

The high deviation of the simulated result from the measured result at low flux density is due to the high measurement sensitivity in this flux density range. The magnetic deterioration (ΔH) is calculated according to Eq. 4.

(4) $$\Delta H\ [\%] = \frac{100 \cdot \left(H_\mathrm{weld} - H_\mathrm{Glued}\right)}{H_\mathrm{Glued}}$$

It depicts increase in field strength (H) to attain a specific flux density. The deterioration is attributed to the high increases in the residual stress and grain size (changes in micro-structure) emanating from the welding procedure. An almost identical maximum percentage degradation of the simulated ($36\,\%$) electromagnetic property of the material compared to the measured ($40\,\%$) result is observed. Fig. 9 shows that there is percentage degradation in unsaturated flux density spectrum in simulation in comparison to the measured result.

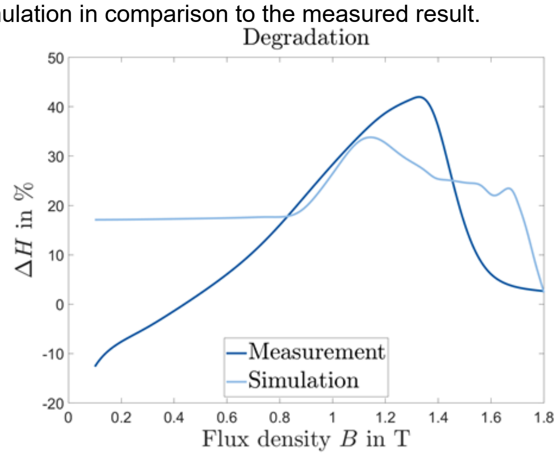

Fig 9: Change of the magnetic field strength.

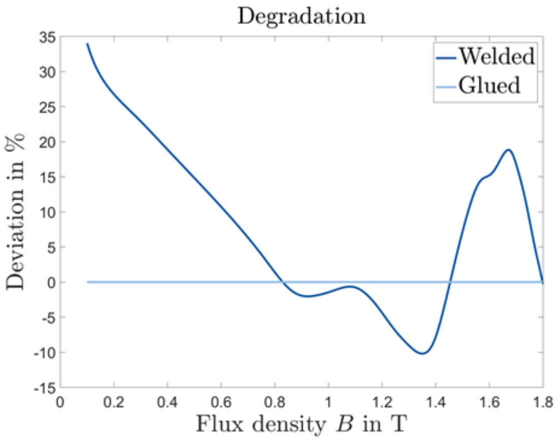

Fig 10: Deviation of the simulation from the measurement.

It shows that the local varying modeling of the electromagnetic property is in good agreement with the measured results.

(5) $Deviation\,[\%] = \frac{100\cdot(H_{\text{Simulation}} - H_{\text{Measurement}})}{H_{\text{Measurement}}}$

Deviations between the measurement and simulation results are mainly due to the interpolation methodology of the look-up table and the calculation of the respective reluctivity values. The calculation is done according to the Froehlich-Kennelly approximation method. An overall good agreement at higher flux density is observed.

Conclusions

For an effective simulation of the effects of weld-packaging, a locally varying material model is developed. This model depicts the electromagnetic property as a function of both residual stress and micro-structure (grain size). Understanding the degree of deterioration with respect to the weld-packaging parameters will enable an efficient improvement of the effects of the weld-packaging on the electromagnetic properties of electric steel. For the modeling of the welding process, an equivalent heat source is utilized in simulating the grain size (changes in micro-structure) and residual stress distribution. The mode of diffusion of the thermal energy is dependent on the modeled weld-packaging parameters. The local varying material model for the simulation are determined from the mapping of the simulated grain size and stress distributions with the electromagnetic measurement of the processed samples annealed. The electromagnetic analysis of the processed samples shows a deterioration of the sample with increasing grain size and residual stress. It can be seen that an up to $100\,\%$ increase in the average grain size will lead to an up to $40\,\%$ reduction of the maximum attainable relative permeability of the material. Observation of an initial improvement of the electromagnetic property is seen with increasing stress, deterioration is observed at stress values higher than $60\,\text{MPa}$. The model verification results show a general deterioration of electromagnetic property due to weld-packaging. This can be attributed mainly to the high increases in the residual stress emanating from the welding procedure. An almost identical maximum percentage degradation of the simulated ($36\,\%$) electromagnetic property of the material compared to the measured ($40\,\%$) result is observed. The high deviation of the simulated result from the measured result at low flux density is because of the higher measurement sensitivity in this flux density range. A more visible deterioration of the magnetization is observed for both simulated and measured ring cores at flux densities between $0.8\,\text{T} - 1.5\,\text{T}$.

Acknowledgment

The work is funded by the Deutsche Forschungsgemeinschaft (DFG) 432930813 in the research group project "Elektromagnetische Bewertung und Quantifizierung von Schweißprozessen zur Paketierung von Elektroblechen".

***Authors**: David Ukwungwu M.Sc, Institute of electrical Machine, Schinkelstraße 4, 52062 Aachen, E-mail: david.ukwungwu@iem.rwth-aachen.de; Dr. -ing. Nora Leuning, Institute of electrical machine, Schinkelstraße 4, 52062 Aachen, E-mail: nora.leuning@iem.rwth-aachen.de; Prof. Dr. -ing. Kay Hameyer, Institute of electrical machine, Schinkelstraße 4, 52062 Aachen, E-mail: hameyer@iem.rwth-aachen.de*.

REFERENCES

[1] Arshad, W. M., Ryckebush, T., Magnussen, F., Lendenmann, H., Soulard, J., Eriksson, B., and Malmros, B.: "Incorporating Lamination Processing and Component Manufacturing in Electrical Machine Design Tools", *IEEE Industry Applications Annual Meeting*, pp. 94–102, 2007.

[2] Leuning, N., Steentjes, S., Gerhards, B., Reisgen, U., Hameyer, K.: "Analysis of a novel laser welding strategy for electrical steel laminations", *7th International Electric Drives Production Conference (EDPC)*, pp. 1–8, 2017.

[3] Leuning, N., Steentjes, S., Hameyer, K.: "Effect of grain size and magnetic texture on iron-loss components in NO electrical steel at different frequencies", *Journal of Magnetism and Magnetic Materials*, vol. 469, pp. 373–382, 2019.

[4] Leuning, N., Steentjes, S., Weiss, H. A., Volk, W., Hameyer, K.: "Magnetic Material Deterioration of Non-Oriented Electrical Steels as a Result of Plastic Deformation Considering Residual Stress Distribution", *IEEE Transactions on Magnetics*, vol. 54, no. 11, pp. 1–5, 2018.

[5] Luming, L., Songling, H., Xiaofeng, W., Keren, S., and Su, W.: "Magnetic field abnormality caused by welding residual stress", *Journal of Magnetism and Magnetic Materials*, vol. 261, no. 3, pp. 385–391, 2003.

[6] Ukwungwu, D., Krichel, T., Schauerte, B., Leuning, N., Olschok, S., Reisgen, U., and Hameyer, K.: "Electromagnetic assessment of welding processes for packaging of electrical sheets", *10th International Electric Drives Production Conference (EDPC)*, pp. 1–6, 2020.

[7] Wang, H., Zhang, Y., and Li, S.: "Laser welding of laminated electrical steels", *Journal of Materials Processing Technology*, vol. 230, pp. 99–108, 2016.